Nonlinear Magneto-Optical Rotation Magnetometers

Wojciech Gawlik and Szymon Pustelny

Abstract Nonlinear magneto-optical rotation (NMOR) is the nonlinear contribution to the overall magneto-optical rotation (Faraday) signal. It yields signals that are dependent on the light and magnetic-field intensities. The later dependence enables precision magnetometry of very weak fields (relaxation-rate limited). The effect may also be investigated with the modulated light (frequency and/or amplitude modulation) to allow accurate measurements of non-zero magnetic fields. The main advantages of the NMOR magnetometry are: technical simplicity, high accuracy and wide dynamic range.

1 Introduction

Magneto-optical rotation is a magneto-optical effect, consisting in the rotation of a polarization plane of linearly polarized light during its propagation through a medium subject to an external magnetic field. The polarization rotation was discovered by M. Faraday in 1845, during his studies of propagation of light through solids [1]. Half a century later, D. Macaluso and O. Corbino investigated the Faraday effect in gases [2, 3]. Their investigations revealed a strong resonance behavior of polarization rotation on the wavelength of propagating light. This discovery was eventually recognized by calling the resonant version of the Faraday effect the Macaluso-Corbino effect [4].

Figure 1 illustrates a principle of the magneto-optical rotation experiment. Resonant, linearly polarized light is used to illuminate a magneto-optically active medium subject to a longitudinal magnetic field $\boldsymbol{B}$. Rotation of the polarization plane $\varphi(B)$ allows measurement of the magnitude of the field.

The Faraday effect results from the magnetic-field induced circular birefringence of a medium (magnetic-field-induced difference in refractive indices n_- and n_+ of

W. Gawlik (✉) · S. Pustelny
M. Smoluchowski Institute of Physics of the Jagiellonian University,
ul. Łojasiewicza 11, 30-348 Kraków, Poland
e-mail: gawlik@uj.edu.pl

S. Pustelny
e-mail: pustelny@uj.edu.pl

A. Grosz et al. (eds.), *High Sensitivity Magnetometers*, Smart Sensors,
Measurement and Instrumentation 19, DOI 10.1007/978-3-319-34070-8_14

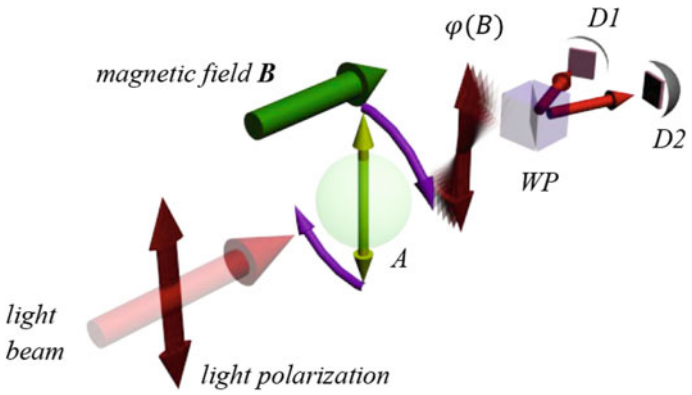

Fig. 1 Schematic of magneto-optical rotation experiment. Resonant, linearly polarized light beam illuminates a magneto-optically active medium (A) subject to a longitudinal magnetic field $\boldsymbol{B}$. Magnetic-field induced rotation of the polarization plane $\varphi(B)$ is measured by a polarimeter composed of a polarizer (WP) and two photodetectors

left- and right-hand circularly polarized light, respectively). The effect links a specific optical property of a material, the Verdet constant V [5], with the magnitude B of the magnetic field $\boldsymbol{B}$ aligned along the light beam. For weak light intensity, i.e. in a linear regime of light-matter interaction, the dependence of polarization rotation on the magnetic field is characterized with a simple proportionality relation [1].

$$\varphi = VLB, \tag{1}$$

where L is the path length of light in the medium. This dependence enables quantification of the magnetic field by the detection of polarization rotation.

Equation (1) shows that magnetometric capabilities of the Faraday effect are determined by the Verdet constant. In solid-state materials, large Verdet constants are observed, for example, in magnetic garnets. In particular, terbium gallium garnet reveals the highest ever-reported Verdet constant of roughly 100 rad/(T m) at 600 nm. Large Verdet constants are also observed in glasses containing high concentrations of lead and bismuth. Unfortunately, the choice of appropriate materials with high Verdet constants and low absorption is rather limited. Therefore, magnetometric sensitivity of a sensor is often increased by prolongation of light propagation length. A specific solution following this approach consists in application of optical fibers containing ferromagnetic dopants [6].

In gases, the situation is different than in solids. Atomic or molecular gases illuminated with off-resonance light typically reveal very small Verdet constants. Therefore, it is very difficult to get measurable rotation signals without application of multipass cells [7, 8] or optical cavities [9]. However, the strong dependence of the Verdet constant on the wavelength results in significant increase in magneto-optical rotation for resonant light, enabling observation of sizeable magneto-optical signals. The transformation between the Macaluso-Corbino and

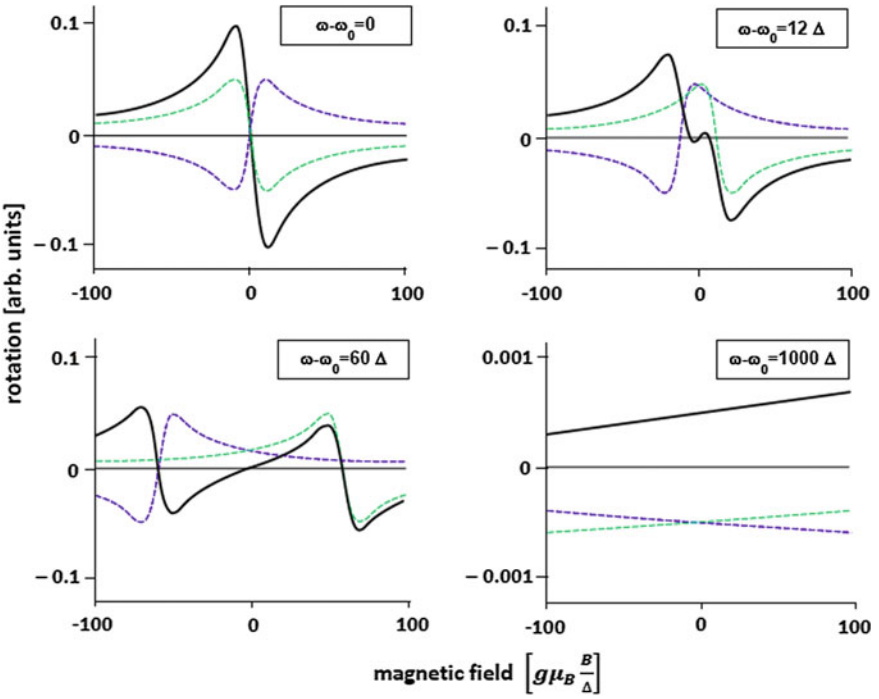

Fig. 2 Transition between the Macaluso-Corbino effect (the resonant Faraday effect) and the Faraday effect (strong detuning). The plots show the magnetic-field dependence of the refractive indices for the left- (*dashed green lines*) and right-handed (*dashed blue lines*) components of the linearly polarized light. Their difference (*solid line*) determines the overall polarization rotation φ. Various panels correspond to different detunings $\omega - \omega_0$. Increasing detuning results in: (i) inversion of sign of the polarization rotation $\varphi(B)$ curve near $B = 0$; (ii) lowering of the rotation amplitude (note the expansion of the vertical scale by factor of 100 in the last plot); (iii) broadening of the linear dependence of φ on B. Magnetic field is expressed in relative units $g\mu_B B/\Delta$, where g is the Lande factor, μ_B is the Bohr magneton, and $\Delta = 10$ is the transition linewidth

Faraday effect is schematically presented in Fig. 2. The figure depicts the refractive indices n_- and n_+ of the left- and right-hand polarization components of linearly polarized light, as well as their difference, determining the polarization rotation φ, as functions of the magnitude of longitudinal magnetic field B

$$\varphi = \frac{\omega}{2}(n_+ - n_-)L, \tag{2}$$

where we used natural units $c = \hbar = 1$. The panels corresponding to various detunings $\omega - \omega_0$, where ω is the frequency of light and ω_0 is the transition frequency, demonstrate the change of the rotation amplitude from the on-resonance excitation (the Macaluso-Corbino effect) to the off-resonance excitation (the Faraday effect). Together with the amplitude reduction, the panels demonstrate

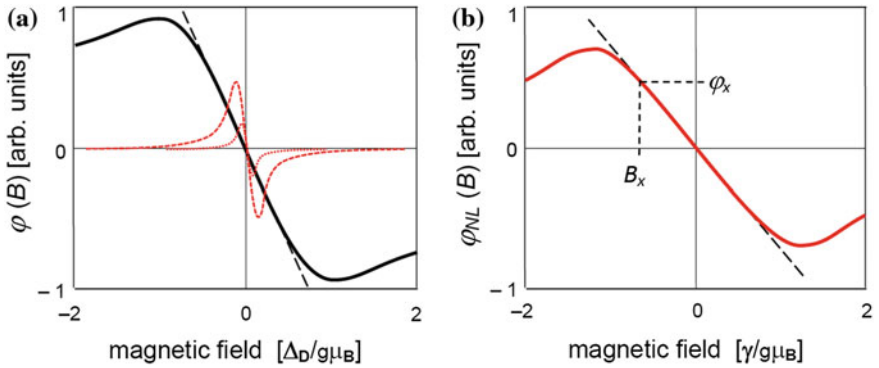

Fig. 3 **a** Schematic illustration of polarization rotation as a function of the magnitude of longitudinal magnetic field, $\varphi(B)$ in the Macaluso-Corbino effect, recorded in a typical inhomogeneously broadened medium (*solid line*). The central part of this dependence, where $\varphi(B)$ exhibits linear dependence (*dashed line*), can be used for determination of the magnetic field. Contribution of the nonlinear rotation adds an intensity-dependent, narrow feature, $\varphi_{NL}(B)$, to the linear rotation (*dotted* and *broken lines* depict contributions for two different light intensities affected by power-broadening). **b** Thanks to the linear dependence of the central part of the narrow $\varphi_{NL}(B)$ contribution associated with the nonlinear Faraday effect, precision determination of the magnetic field B is possible from the measurement of the rotation angle φ. Note the horizontal scale difference between (**a**) and (**b**) which reflects the difference between the Doppler width Δ_D and relaxation rate γ of the ground-state coherence

widening of the magnetic-field range where relation (1) can be applied for measurement of the magnetic field.

Despite the difference in the dependence of the magneto-optical rotation on the magnetic field in the Faraday and Macaluso-Corbino effects, in each case there is a finite magnetic-field range around $B = 0$, which, according to Eq. (1), reveals a linear dependence on the field (broken line in Fig. 3a). Such linearity is very convenient for magnetometry, the polarization rotation provides information about the magnitude of the field B and the steepness of the dependence $(d\varphi/dB|_{B=0})$ determines sensitivity of weak-field measurements (Sect. 3.1). For low light power, the rotation amplitude and the linearity range are limited by the linewidth of the transition light acts on. In solids, where the linewidths may be as large as tens of nanometers, the linearity range is large, but for sensors based on atomic/molecular gases the typical width is on the order of a Doppler width Δ_D (on the order of a gigahertz), which corresponds to the measurement range significantly smaller than one tesla ($\Delta B \lesssim 0.1\,\mathrm{T}$). Consequently, for such sensors the deviations from the linear dependence are observed already at moderate magnetic fields. When the magnetic-field splitting of the resonance line exceeds the linewidth, the rotation decreases and, more importantly, cannot be unambiguously attributed to a specific value of a magnetic field.

The development of techniques of optical pumping [10] and sensitive methods of radio-frequency spectroscopy [11, 12] in 1950–1960 triggered a substantial progress in optical magnetometry (see other chapters of this book). However, it was the advent of tunable lasers that boosted the development of the techniques based

on magneto-optical rotation. One of early studies of the Macaluso-Corbino effect with laser light was performed in the forward-scattering geometry, where transmission of light through a magneto-optically active medium placed between two crossed polarizers was detected (the signal in the arrangement is given by $S \propto I_0 \sin^2 \varphi(B)$, where I_0 is the intensity of light) [13]. The authors of Ref. [13] discovered that when the light intensity is not very low, the polarization-rotation dependence differs, in its central part (around $B \approx 0$), from the standard low-intensity signal $\varphi_L(B)$ (Fig. 3). In particular, a narrow structure arises with the amplitude depending on the light intensity, which reveals nonlinear character of the effect. The nonlinear contribution of the overall magneto-optical rotation signal is denoted as $\varphi_{NL}(B)$ and the related effect is called nonlinear magneto-optical rotation (NMOR). It should be stressed that the range where this feature appears is not subject to Doppler broadening but is determined by the relaxation rate of the atomic/molecular ground state that is coupled with light. Since the rate is orders of magnitude smaller than the Doppler width, even with somewhat smaller rotation amplitude than in the linear effect, the steepness of the polarization-rotation is much larger than in the linear effect ($d\varphi_{NL}/dB \gg d\varphi_L/dB$). Consequently, the sensitivity of NMOR to the magnetic field is much higher than in its linear counterpart. This enhancement can be exploited for magnetometry, as shown in Fig. 3b, albeit in a correspondingly narrower magnetic-field range. Section 2.2 describes the measurements without compromising on the field range.

2 Physical Grounds of Nonlinear Magneto-Optical Rotation (NMOR)

2.1 DC Light

There are several effects that contribute to NMOR signals. The underlying effects behind the phenomenon are associated with redistribution of atomic populations by velocity-selective optical pumping (the Bennet effect [14]) and atomic polarization of a ground state (redistribution of atomic population of the state and generation of coherence between its Zeeman sublevels) [4, 15, 16]. Some of these contributions can be distinguished in the magnetic-field domain as they typically give rise to optical rotation that peaks at different magnetic fields, leading to a group of dispersive features nested around $B = 0$. In general, the width of the narrowest feature is determined by the ground-state coherence relaxation rate γ, which is inversely proportional to the transverse relaxation time T_2.

To understand the basic principles of this relation and limitations of traditional[1] (dc) NMOR for the detection of weak magnetic fields, it is instructive to consider a simple $J = 1 \rightarrow J' = 0$ atomic system resonantly coupled by linearly-polarized

[1]Using unmodulated light.

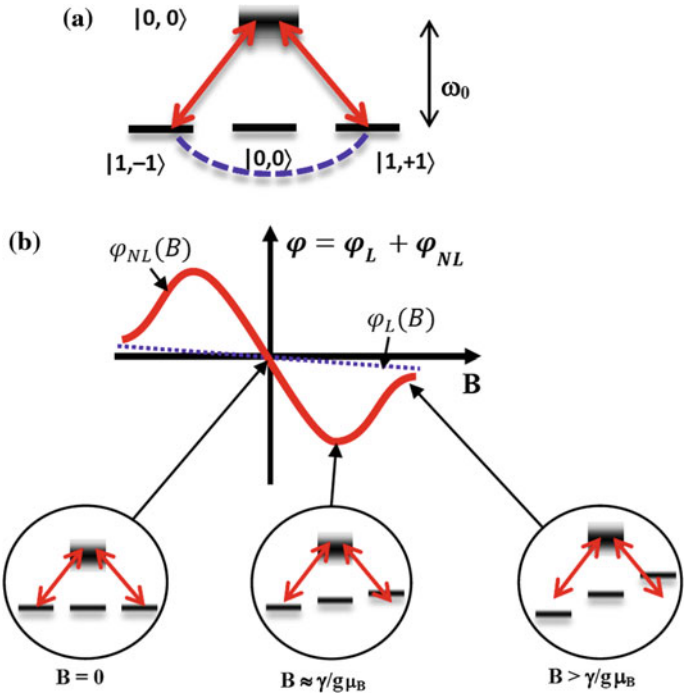

Fig. 4 Schematic illustration of the creation of the coherence contribution to NMOR. **a** Linearly-polarized light creates Raman coupling of the ground-state sublevels $|1, \pm 1\rangle$ via the excited state $|0, 0\rangle$ (ground-state coherence marked by *blue dashed line*). **b** atomic coherence between states $m_J = \pm 1$ (not shown in *insets*) is responsible for the additional contribution $\varphi_{NL}(B)$ to the overall rotation (*red line*) which is narrower than the contribution of the linear polarization rotation $\varphi_L(B)$ (*dotted line*). The *insets* represent the creation of the coherence for three characteristic values of the magnetic field intensity, $B = 0$, $B \approx \gamma/(g\mu_B)$, and $B > \gamma/(g\mu_B)$

light. If the light propagates along the quantization axis z, its linear polarization is a superposition of two circular polarizations σ^+ and σ^-, which excite transitions according to specific selection rules (the σ^+-polarized light excites transitions with $m_{J'} - m_J = 1$, where m_J and $m_{J'}$ are the magnetic quantum numbers of a ground and excited state, respectively, and the σ^--polarized light excites transition with $m_{J'} - m_J = -1$). Thereby, in the $J = 1 \rightarrow J' = 0$ system, the light coherently couples the $|1, \pm 1\rangle$[2] ground-state sublevels with the $|0, 0\rangle$ excited-state sublevels, generating the superposition of ground-state sublevels with $\Delta m = 2$ (represented in Fig. 4a by a dashed line). In zero magnetic field, the ground-state sublevels are degenerate, thus the light-established coherence has maximal amplitude but the coherence is stationary (the same energy of the sublevels ensures absence of the coherence evolution).

[2]We label the states as $|J, m_J\rangle$.

Despite the maximal amplitude of the coherence, a perfect symmetry in the propagation of σ^+ and σ^- components of light at $B = 0$ ensures absence of the phase shift between the beams and hence no polarization rotation, $\varphi(0) = 0$. For non-zero fields, $B \neq 0$, the Zeeman sublevels are split (sublevel energy shift is given by $E_Z^m = m\omega_L$, where $\omega_L = g\mu_B B$ is the Larmor frequency). Consequently, the superposition becomes nonstationary, i.e., its phase oscillates with a frequency $2\omega_L$.[3] Competition between generation of the coherence and its precession reduces the amplitude of the net coherence and changes its phase depending on the magnetic-field. Although the amplitude of the light-generated coherence at $B \neq 0$ is smaller than that established at $B = 0$, the different phase shift of the two circular components of light leads to non-zero polarization rotation. The polarization-rotation angle depends on the amplitude of the coherence, determined, for example, by light intensity and tuning, but also by the magnetic field. For instance, for $|B| < \gamma/(g\mu_B)$ the rotation linearly depends on the magnetic field, reaching its extreme value for $|B| = \gamma/(g\mu_B)$ and deteriorating for stronger fields. This is due to the further decrease of the amplitude of generated coherence. Figure 4b schematically shows the characteristic features of the NMOR signal along with the corresponding physical system.

While the first manifestation of NMOR was in the forward-scattering experiment, the recorded NMOR signals even though of subnatural width (narrower than the relaxation rate of the excited state) were still relatively broad (hundred-nanotesla range). In 1998, D. Budker and coworkers investigated NMOR, demonstrating signals with a width of roughly 10^{-10} T [17]. These signals allow for a magnetic-field sensitivity of 10^{-15} T/Hz$^{1/2}$ detectable in a dynamic field range of roughly 10^{-10} T. While this is one of the highest sensitivity ever demonstrated, the narrow dynamic range is one of the largest problem of the technique.

2.2 Modulated Light

A significant step in alleviating the limitation of the dynamic range to fields close to $B = 0$, was the application of modulated light for synchronous pumping of atoms. This idea goes back to the seminal work of Bell and Bloom [18] who discovered that modulation of light enables generation of dynamic (time varying) spin polarization of a medium. Specifically, the authors showed that intensity modulation of circularly-polarized light with frequency ω_m allows observation of a resonance in light absorption; the reduced absorption is observed if the modulation frequency coincides with the Larmor frequency, $\omega_m = \omega_L$. Synchronous optical pumping, which the Bell-Bloom experiment is an example of, can be also realized with linearly polarized light. To understand NMOR when modulated light is used, it is instructive to consider the system in the frame rotating with the modulation

[3] In general, the evolution frequency ω_{coh} is given by $\omega_{coh} = \Delta m \omega_L$.

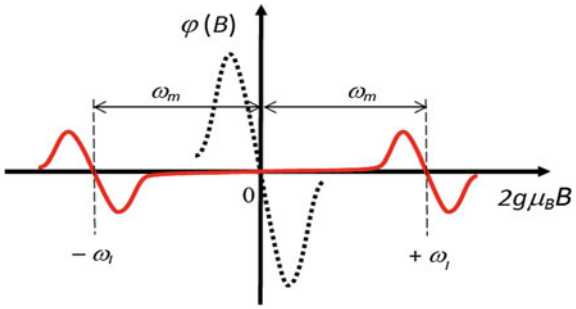

Fig. 5 Modulation of pumping creates dynamic/modulated NMOR signals allowing measurements of nonzero magnetic fields. The measurement accuracy of the stronger, nonzero fields is close to what dc NMOR offers in the low-field region (depicted by the *black dotted line*) yet thanks to the modulation of the pumping rate the measurements may be extended to higher fields. When the modulated rotation signal is retrieved by a lock-in detector, the signal consists only of the two side components centered at $\pm\omega_m/(2\,g\mu_B)$ (*red solid line*)

frequency ω_m. Since modulated light can be decomposed into two counter-rotating components, $\pm\omega_m$, for a given magnetic field, one of the components rotates with the frequency close to the spin-precision frequency (coherence-evolution frequency), while the other is strongly off-resonant and hence its contribution to coherence generation is negligible. As described above, in NMOR the coherence evolution frequency is given by $2\omega_L$, thus for the frame rotating with $\omega_m \approx 2\omega_L$, NMOR with modulated light is equivalent to dc NMOR. Figure 5 illustrates how the existence of two counter-rotating components of modulated light results in resonant generation of the ground-state coherence when

$$B = \pm\frac{\omega_m}{2g\mu_B}. \tag{3}$$

The relaxation rate of the coherence generated with modulated light is determined by the ground-state coherence relaxation rate γ, similarly as in the dc case. Hence, in the first order, the zero-field NMOR signal and the signal with modulated light have same widths. As the modulation frequency can be varied, the position of the high-field NMOR resonance can be precisely controlled (Eq. 3). This opens the possibility to detect stronger magnetic fields and extend the dynamic range to the fields exceeding the Earth's magnetic field. It should be noted, however, that at stronger fields, the high-field NMOR signal deteriorates due to the nonlinear Zeeman effect [19], alignment-to-orientation conversion [20], nonlinearities of the magnetic field, etc. This deterioration sets a practical limit on the dynamic range of NMOR with modulated light.

In principle, any quantity that affects the light-atom interaction can be used as a source of modulation in synchronous pumping. In the case of magnetometers based on magneto-optical rotation, two techniques are used most often: the frequency modulation (FM NMOR) and amplitude (or intensity) modulation (AMOR) [21].

A thorough analysis of methods based on other modulation schemes has been recently published by Weis et al. [22, 23].

2.2.1 FM NMOR

The FM NMOR technique employs frequency-modulated (FM) light with its electric field depending on time as [24]

$$E = E_0 \cos(\omega(t)t) = E_0 \cos\left(\omega^{(0)} + \Delta\omega \cos\omega_m t\right)t \tag{4}$$

where $\omega^{(0)}$ is the carrier frequency and $\Delta\omega$ is the modulation amplitude. The described modulation of the light-beam modulates the pumping rate of atoms (Fig. 6a shows the concept of FM optical pumping using the $F = 2 \rightarrow F'$ transitions of the rubidium D_1 line , i.e. a system often used in NMOR). If ω_m is resonant with twice the Larmor frequency, $\omega_m = 2\omega_L$ (Eq. 3), atoms are synchronously pumped, maximum dynamic polarization is induced and modulated component of the polarization rotation reaches its maximum, i.e., the FM NMOR resonance is observed.

Figure 6b shows a typical FM NMOR signal measured versus the modulation frequency for a given magnetic field ($B \approx 1.8$ μT). The NMOR signal was measured with an unmodulated light beam whose polarization rotation was detected with a lock-in amplifier operating at the first harmonic of the modulation frequency (see Sect. 4.2.1 for more details). The two curves correspond to the two component of the signal: the dispersive in-phase component (solid blue line) and the quadrature component (dashed red line). For a given set of parameters, the amplitude of the

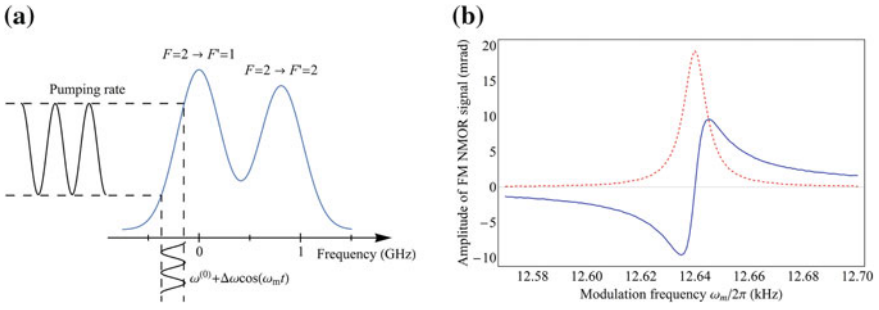

Fig. 6 **a** Schematic of the mechanism of modulation of pumping rate using FM light. The plot shows a case of light tuned to the $F = 2 \rightarrow F'$ transitions of the Doppler-broadened rubidium D_1 line (often used for NMOR magnetometry) with frequency modulated on a slope of a Doppler broadened transition. The scheme depicts how the frequency modulation of light (horizontal modulation) leads to the modulation of the pumping rate of atoms. **b** The in-phase and quadrature components of a typical FM NMOR signal measured in rubidium vapor contained in paraffin-coated cell. The signal was recorded for light intensity of roughly 1 mW/cm^2 tuned to the low-frequency slope of the $F = 2 \rightarrow F' = 1$ transition of the rubidium D_1 line with $\Delta\omega \approx 2\pi \times 100\,\mathrm{s}^{-1}$

recorded signal is equal to about 20 mrad, while its width is about 30 Hz (measured peak-to-peak).

Figure 6b illustrates that the FM NMOR resonance occurs at nonzero magnetic field. When the field changes, the resonance position can be retrieved by corresponding change of the modulation frequency ω_m, which enables magnetometry beyond the $B \approx 0$ limit of dc NMOR.

2.2.2 AMOR

The AMOR technique employs modulation of the amplitude (AM) of the light field used for the experiment. For detection of the modulation signal the same procedure as in the case of FM NMOR is used, with lock-in detection of the time-dependent rotation detected at the harmonic of the modulation frequency [25].

An example of AMOR signal is shown in Fig. 7. Similarly as for FM NMOR, a strong resonance is observed when light modulation frequency coincides with twice the Larmor frequency. The signal was measured in the same cell as the signal presented in Fig. 6, however, different tuning, average light intensity and magnetic field lead to slightly broader resonance of larger amplitude occurring at $\omega_m \approx 29.3$ kHz.

All modulators used for AMOR technique modulate the light intensity I,

$$I(t) = \frac{I_0}{2}(1 + \mathrm{A}\,\cos\omega_m t), \tag{5}$$

where A is the modulation amplitude. That simple modulation technique yields very conveniently detection signals. The theoretical analysis, however, addresses the

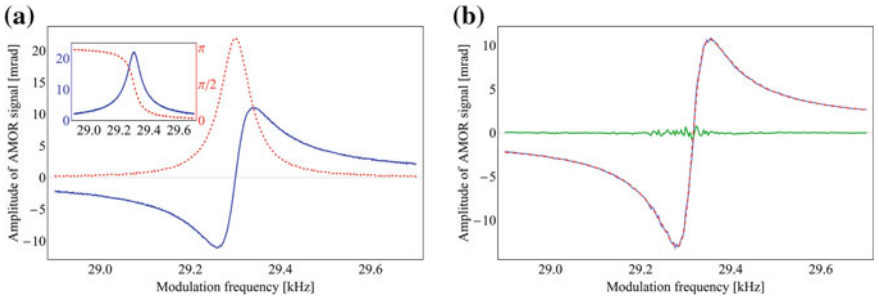

Fig. 7 **a** Typical AMOR signal measured in-phase (*solid blue*) and quadrature (*dashed red*) with the modulation frequency at its first harmonic. *Inset* shows the corresponding amplitude (*solid blue*) and phase (*dashed red*) of the AMOR signal. **b** In-phase AMOR signal (*solid blue*) overlaid with the fit to the dispersive Lorentz function (*dashed red*) and the data-fitting difference signal (*solid green*). The AMOR signal was recorded in paraffin-coated cell with sinusoidally modulated light (100 % modulation depth), average light intensity of 1 mW/cm^2, and light tuned to the center of the $F = 2 \rightarrow F' = 1$ transition of the rubidium D_1

electric field amplitude, rather than the light intensity. For the 100 % modulation, $A \approx 1$, in which case the relation for the amplitude of light field ($E = \sqrt{I}$) yields

$$E(t) = \frac{E_0}{2}\left[\cos\left(\omega - \frac{\omega_m}{2}\right)t + \cos\left(\omega + \frac{\omega_m}{2}\right)t\right]. \tag{6}$$

As will be discussed in more details later in this chapter, FM NMOR method is very easily applicable thanks to the possibility of using diode lasers where FM can be easily accomplished by modulating the diode-laser current. At the same time, however, current modulation is associated with modulation of the light intensity, so a pure FM modulation becomes difficult or even impossible. In such cases the AM technique is more recommended.

3 Characteristics of Optical Magnetometers

3.1 Sensitivity

3.1.1 Fundamental Limits on the Sensitivity

One of the most important parameters of a magnetometer is its sensitivity. In optical magnetometers, the fundamental limit on the sensitivity stems from the quantum nature of objects involved in magnetic-field sensing as well as coupling between them. Since the contributions from the atoms, photons, and atom-photon interaction are independent, the fundamentally sensitivity limited δB_f may be written as

$$\delta B_f = \sqrt{\delta B_{at}^2 + \delta B_{ph}^2 + \delta B_{ba}^2}, \tag{7}$$

where δB_{at} is the sensitivity limit due to the atoms, δB_{ph} is the photon-limited sensitivity, and δB_{ba} is the limit due to the action of the probing light onto the atoms.

The atomic limit on the sensitivity originates from the Heisenberg uncertainty principle on spin projections

$$\delta F_i^2 \delta F_j^2 \geq \frac{\left|\left\langle \left[F_i, F_j\right]\right\rangle\right|^2}{4} = \frac{\langle F_k\rangle^2}{4}, \tag{8}$$

where $F_{i,j,k}$ are three components of the spin $\boldsymbol{F}$ and [,] denotes the commutator. For the coherent spin states [26], inequality (8) is saturated and the projection-noise-limited magnetic-field sensitivity δB_{at} may be written as [27]

$$\delta B_{at} = \frac{1}{g\mu_B}\sqrt{\frac{1}{N_{at} T_2 \tau}}, \tag{9}$$

where N_{at} is the total number of atoms involved in light-atom interaction, T_2 is the transverse relaxation time (the spin-coherence lifetime), and τ is the duration of the measurement. According to Eq. (9), the sensitivity depends on the number of atoms N_{at}, the relaxation time T_2, and the measurement time τ. This dependence reveals potential strategies for improving the sensitivity, which consist in improving the measurement time or increasing the $N_{at}T_2$ product. The limitation of the first approach is a finite bandwidth required in many measurements or necessity of providing good temporal stability of such parameters as magnetic field or light intensity/frequency. The second approach requires increasing the number of atoms involved in the field detection (achievable, for example, by rising atoms' density n_{at} via vapor temperature) or by increasing the transverse relaxation time T_2. In typical NMOR magnetometers, where magneto-optically-active vapors are contained in volumes smaller than 10 cm^3, the magnetic-field sensing is performed at room or slightly alleviated temperatures (typically lower than 60 °C). This condition is set by the desire to operate with media of optical depths on the order of unity, which optimizes the spin-polarization process (optical pumping) and hence the sensing performance on NMOR magnetometer. In particular, at higher depths/concentrations, such processes as radiation trapping [28] and spin-exchange collisions [29] become important sources of relaxation, limiting the sensitivity of NMOR magnetometer. Therefore, to further increase the sensitivity, one needs to prolong the transverse relaxation time T_2. In NMOR magnetometers, T_2 is limited by light-matter effective-interaction time. In evacuated vapor cells, this time is determined by the (effective) time of flight of atoms across the light beam [30, 31] but it can be prolonged either by coating cell walls with a special anti-relaxation layer or by introduction of a buffer gas into the cell. While putting the special (e.g. paraffin) layer on the walls may prevent atoms from depolarizing collisions with the wall, introduction of the buffer (typically noble) gas into the cell slows down the diffusion of atoms toward the walls (the collisions between alkali and buffer-gas atoms preserve, to the first order, the ground-state polarization). These two approaches enable to prolong the relaxation time T_2: up to 10 ms in the buffer-gas cells [32] and over 60 s in the paraffin-coated cells [33]. Although the difference between the times seems to imply the application of anti-relaxation coating, there are additional differences between the approaches that may favor application of a buffer gas (e.g., the ability to operate at higher temperature, spatial sensitivity of the field detection, etc.).

The second contribution to the fundamental limit of the magnetic-field sensitivity is related with the nature of photons. Photons, as quantum particles, obey the Poissonian statistics, which states that their flux per unit time fluctuates over time around its mean value $\bar{N}_{ph}$ with the amplitude $\bar{N}_{ph}^{1/2}$. Consequently, the intensity and polarization of light can be determined with a finite precision given by $\left(\bar{N}_{pr}\tau\right)^{-1/2}$, where $\bar{N}_{pr}$ is the number of probe-light photons. This sets a limit on the precision of spin-state determination and hence the sensitivity of magnetic-field measurements. To alleviate this problem, one can operate with higher probe-light intensities, where

the signal-to-noise ratio increases[4] and hence does the magnetic-field sensitivity. With such increased intensity it was possible to reach the shot-noise limit over a wide magnetic-field range from 5 to 75 μT with AMOR magnetometer [34]. It should be noted, however, that for more intense probe light, optical pumping with probe becomes an important process. Thus, to reduce this effect, one may detune the probe beam from the transition. In that case, the photon shot-noise limited sensitivity δB_{ph} improves due to the increase in $\bar{N}_{pr}$, while the medium is still weakly affected (absorption on an isolated transition scales as $1/\Delta^2$, while dispersion as $1/\Delta$, where Δ is detuning).

The final contribution limiting the magnetic-field sensitivity arises from the back-action of probe light onto the atoms. This contribution originates from the ac Stark shift, the effect, consisting in the modification of Zeeman-sublevel energies by an electric field of light. This modification leads to the change of spins' precession frequency, mimicking the change of the external magnetic field. Thereby, the fundamental fluctuations in light intensity may contribute to the uncertainty of the spin-state determination and hence limit the sensitivity. Consequently, reduction of the back action becomes an important issue in optical magnetometry. Several approaches to reduce the back action have been reported in the literature [34–37]. Among them, a popular strategy based on detuning of the probe light from an optical transition seems particularly appealing [38]; for large detunings, the Stark shift scales inversely proportional to the square of the detuning, thus operation under such conditions allows one to significantly reduce the back-action contribution to the sensitivity. By an appropriate choice of a magneto-optically active medium and an appropriate choice of operation conditions (gas temperature, transverse relaxation limiting techniques, pump- and probe-light intensities and detunings, etc.), the fundamental limit on the sensitivity of NMOR magnetometer can reach or even surpass 1 fT/Hz$^{1/2}$. In particular, the low-field NMOR magnetometer discussed in Ref. [39] reveals the fundamental sensitivity of 0.16 fT/Hz$^{1/2}$, while its high-field counterpart, exploiting intensity-modulated light, had a sensitivity on the order of 10 fT/Hz$^{1/2}$ [40, 41].

3.1.2 Technical Limits on the Sensitivity

While three contributions described above set the fundamental limit on the sensitivity of NMOR magnetometers, practical devices are typically characterized with worse performance. The sensitivity deterioration stems from non-ideal conditions under which the devices are being operated. In real world, technical factors increase the noise, which impairs the sensitivity of the magnetometer.

[4]Neglecting optical pumping of atoms by the probe light, the NMOR-signal amplitude scales linearly with the number of probe-light photons (the signal is $S = I_{pr} \sin^2 \varphi$), while the noise/uncertainty is proportional $\sqrt{I_{pr}}$.

A particular source of technical noise in optical magnetometers are fluctuations in light-propagation conditions. In real systems, vibrations of optical elements and air turbulences change phase, intensity, and spatial profile of light interacting with the magneto-optically-active medium. This may affect the light-matter coupling and/or efficiency of light detection. Thermally-induced drifts of optical or mechanical properties of components used in the magnetometers may also affect the interaction between light and matter and hence contribute to the noise. Another source of noise is electronics, which may contribute to the sensitivity loss via photodetector dark current, electromagnetic (e.g., ac) pickups, or thermal instabilities of electronic equipment. In contrast to the fundamental noise, however, most of these contributions is frequency dependent. Figure 8 shows a typical noise spectrum of the NMOR magnetometer. As seen, the spectrum reveals a $1/f$-dependence with clearly visible harmonics of the ac line (50 and 100 Hz). Such characteristics suggest approaches aiming at reduction of the technical-noise. Specifically, operating the device at higher frequencies reduces the technical-noise contribution. This may be achieved either by modulation of the probe light and its phase-sensitive detection (see Sect. 4.2.1) or by operation of the device in non-zero magnetic fields. The later approach may only be achieved with the devices of sufficiently broad dynamic ranges (Sect. 5). It should be noted, however, that while the contributions from technical noise may be small, they will always impart the performance of NMOR magnetometers.

Independently of the technical-noise contribution, the NMOR magnetometer can also suffer from the magnetic noise present in the detection region of the magnetometer. While, strictly speaking, magnetic-field instability is not "the intrinsic noise" of the magnetometer, it is a factor determining the magnetometric performance of the device (uncontrollable magnetic-field fluctuations may significantly hamper the magnetometer ability to detect small changes of the field).

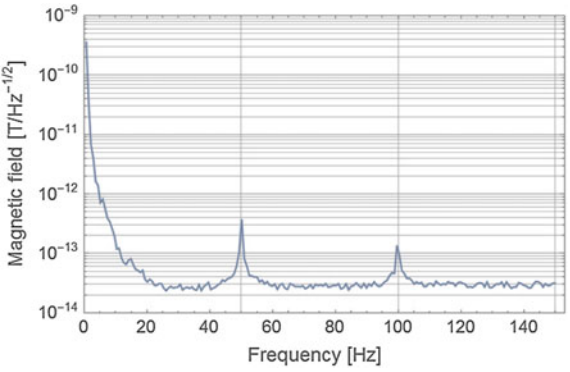

Fig. 8 Noise spectrum of the NMOR magnetometer operating at $B \approx 0$. The spectra reveal a $1/f$-dependence with clearly visible noise peaks at the harmonics of the ac line (50 Hz). In the presented case, the fundamental noise limit is roughly an order of magnitude smaller than the noise floor recorded with the spectra. The difference arises most likely due to the fluctuations of the detected magnetic field

To address this problem, various approaches may be undertaken. One group of the approaches is based on shielding (passive or active) of the external magnetic fields, which enables detection of the field in quieter magnetic-field environment. The passive shielding is typically realized inside magnetic enclosures made of high permeability materials [42]. Particular examples of such enclosures are multilayer mumetal magnetic shields, which typically offer shielding factors at the level larger than 10^4 (depending on the number of layers, geometry, size, etc.). Alternatively, one can use a set of magnetic-field coils to compensate the external fields. This technique enables active compensation of field's drifts as well as fluctuations of the external magnetic fields. To realize such active compensation, an error signal providing a measure of the compensation, is required. Such signal is often provided by non-optical sensors (e.g., flux-gate magnetometers or magneto-resistive sensors), which offer worse magnetic performance (particularly, less sensitive) but are easier to be handled.

An alternative technique of reducing environmental magnetic noise is based on the so-called magnetic gradiometer [43]. In such mode, readouts of two magnetometers placed in series with a source of measured weak magnetic field are being subtracted. As the background field exhibits relatively high spatial uniformity[5] and the magnetic field from the weak source is characterized with a strong distance dependence (r^{-q}, where $q \geq 1$), the separation of the two magnetometers (typically comparable to the source dimensions) ensures that the readout of one of the magnetometers is dominated by the weak source. The difference signal allows reduction of the environmental noise and more accurate measurement of the magnetic field produced by the weak source. Typically, the noise in the gradiometer mode can be reduced by more than an order of magnitude [44].

3.1.3 Sensitivity of Optical Magnetometer

From the practical standpoint, the sensitivity of the NMOR magnetometer is determined by the signal-to-noise ratio (SNR) of the measured NMOR signal; to determine the ability to detect weak magnetic fields, one first needs to determine the slope of the NMOR resonance as a function of the magnetic field and then recalculate the noise into the amplitude of rotation into magnetic-field-determination uncertainty

$$\delta B_{pr} = \frac{\delta\varphi}{\delta B}\frac{N}{S}, \tag{10}$$

where $\delta\varphi/\delta B$ is the slope of the NMOR resonance in its central part. This dependence determines the experimentally detected sensitivity of the magnetic-field

[5]It is typically assumed that the background field is produced by distant sources, so that change of the magnetic field between two magnetometers is negligible.

measurement achieved for a specific set of experimental parameters, including light intensity, tuning, lock-in time constant, etc. To some extent, the optimum conditions depend on one another, but also on environmental conditions (e.g., magnetic-field noise). For this reason, the practical optimization of the sensitivity of the magnetometer requires careful choice of the parameters.

3.2 Bandwidth

Bandwidth is another important characteristic of the optical magnetometer. For a typical optical magnetometer, the response of the magnetometer to small magnetic-field changes is equivalent to a response of a first-order low-pass filter with the time constant T_2 [45]. In turn, for $T_2 < \tau$, the magnetometer bandwidth is determined by $(2\pi T_2)^{-1/2}$, while for shorter measurement times $(T_2 > \tau)$, the bandwidth is given by $(2\pi T_2)^{-1}$. Therefore, to increase the bandwidth one may increase light intensity, vapor temperature or introduce the inhomogeneous magnetic field, which all may shorten the relaxation time T_2. It should be stressed, however, that due to the dependence of the sensitivity and bandwidth on the same parameter T_2, its adjustment needs to be a compromise between sensitivity and bandwidth.

3.3 Dynamic Range

In traditional NMOR magnetometers, i.e., the magnetometers exploiting CW light (Sect. 2.1), not only the sensitivity and bandwidth, but also the dynamic range ΔB_{CW} is limited by the transverse relaxation time T_2, $\Delta B_{CW} = 1/(g\mu_B \pi T_2)$. As shown in Fig. 3, this stems from the dispersive shape of the zero-field NMOR signal, which reveals a linear dependence on the magnetic field only within the range from $-\Delta B_{CW}/2$ to $\Delta B_{CW}/2$. Fields stronger than $|B| > \Delta B_{CW}/2$ cannot be distinguished from the weaker ones (see Fig. 3).

As noted in Sect. 2, to expand the dynamic range of the NMOR magnetometer, one may use modulated light. In that case, the range is not limited by the width of the NMOR signal because the position of the high-field NMOR resonance follows the magnetic field and can be adjusted by changing the modulation frequency (Eq. 3). To the first order, the dynamic range ΔB_{mod} of the modulated NMOR magnetometers is unlimited. In practice, however, the strongest fields measurable with the magnetometers rarely exceed the Earth's magnetic field. This originates from the fact that higher-order effects (e.g., nonlinear Zeeman effect [19], alignment-to-orientation

conversion [20]) diminish the amplitude of NMOR resonance. Also, it is much harder to provide good spatial homogeneity of stronger fields.[6]

3.4 Operation Modes

There are two modes of detection of stronger magnetic fields using NMOR magnetometers. In the first, so-called passive mode, magnetic field is detected by demodulating the magnetometer's output signal (polarization rotation) at the modulation frequency. This allows extraction of the amplitude and phase of the signal. Since in resonance (e.g., for $\omega_m = 2\omega_L$), two characteristics of the signal take specific values (maximum rotation and 90° phase shift), application of a feedback loop controlling the modulation frequency and tracking the resonance position enables measurement of the magnetic field. The phase-sensitive detection allows strong noise suppression (better SNR) and hence more precise tracking of the magnetic field in a broad dynamic range.

Alternatively to the passive mode, the magnetometer can be operated in the self-oscillating mode. In such an arrangement, the magnetometer's output signal is filtered and amplified and then used to modulate light. The dependence of the signal on the modulation frequency (Eq. 3) ensures that from the whole noise spectrum of the signal the system promotes only a specific modulation frequency, i.e., the resonance frequency $(\omega_m = 2\omega_L)$. Moreover, since there is no delay in the response of the spin precession to a magnetic-field change, the system instantaneously adjusts modulation frequency so that $\omega_m = 2\omega_L$. In such a way, the system automatically tracks magnetic-field changes and the modulation frequency provides information about the magnetic field. Moreover, in the self-oscillation mode the width of the NMOR signal may be narrower. This is due to the fact that in the self-oscillating mode the fluctuating magnetic field appears as sidebands to the main frequency determined $2\omega_L$ and can be easily filtered out, while in the passive mode they lead to the broadening of the resonance.

3.5 Scalar/Vector Sensor

In general, NMOR magnetometers are scalar sensors, i.e., they are sensitive to magnitude of the magnetic field. However, a scalar magnetometer can be easily converted into a vector magnetometer by introducing modulation of the magnetic field in three transverse direction at distinct modulation frequencies. Detection of the signal at those frequencies provides information about the magnetic field

[6]The magnetic-field inhomogeneity causes broadening of the observed NMOR resonance and hence deterioration of the magnetometric sensitivity of the device.

components in various directions. Alternatively, the measurement of the field direction may be obtained by the detection of the rotation signal at two frequencies: ω_L and $2\omega_L$. As shown in Ref. [46], the amplitudes of the signals measured at those frequencies depend on the direction of the magnetic field such that their ratio provides information about the direction of the field in the plane perpendicular to the polarization of the incident (probe) light.

3.6 Power Consumption

A particular advantage of optical magnetometers with respect to widespread SQUID magnetometers, that is, the devices of comparable sensitivity, is their low power consumption. In NMOR magnetometers, heating of atomic vapor cell is the most important contribution to the overall energy budget of the system. Modern lasers, particularly, vertical cavity surface emitting lasers (VCSELs), and electronic systems have low power consumption. Consequently, the whole system, without the heating, can be characterized with power demands smaller than 10 W.

4 NMOR Magnetometer Setup

Figure 9 shows a generic setup of a high-field NMOR magnetometer. The system consists of two main parts: optoelectronic part, which contains all light processing and sensing elements and electronic part that contains all elements used in electrical-signal processing.

4.1 Optics and Optoelectronics

The aim of the optoelectronic part of the system is to: (1) generate light with appropriate properties (intensity, wavelength, polarization, temporal characteristics, etc.), (2) couple the light with atomic vapor to effectively optically pump the medium, and (3) characterize the polarization state of the probe light. Below, we describe the means to achieve these aims in more details.

4.1.1 Light Sources

In all NMOR magnetometers, diode lasers are used. From the point of view of optical magnetometry, the diode lasers offer several advantages: tunability, narrow linewidth (<10 MHz for a single-mode laser), and sufficient light power ($\sim$100 μW) of the emitted light. The lasers are also characterized with small sizes,

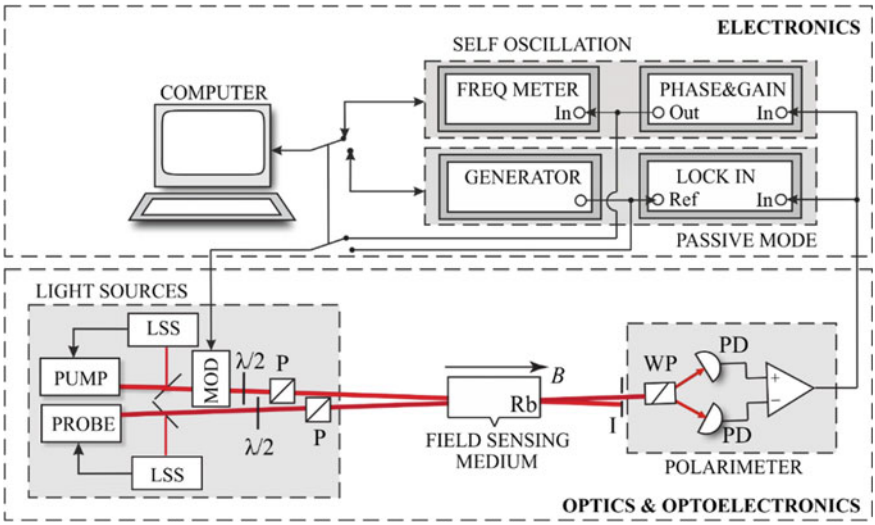

Fig. 9 Generic scheme of the NMOR magnetometer. The upper part represents the electronic part of the system. It contains elements required for operation in the self-oscillation mode (phase shifter, amplifier, frequency meter), as well as elements for the passive mode (lock-in amplifier, generator) along with the computer controlling the whole experiment. The lower part is the optoelectronic part of the system. It contains two lasers (pump and probe), light-wavelength control and stabilization systems (LSS), a light modulator (MOD) placed in the pumping-beam path, vapor cell filled with a magneto-optically-active medium (e.g., Rb), and a polarimeter to detect the polarization state of light. Additionally the system contains a set of optical elements: P and WP stand for polarizers (WP is the Wollastone prism specifically used in the system), PD denotes the photodiodes, $\lambda/2$ is the half-wave plate

low power consumption, good reliability, and possibility of integration with optoelectronic components.

In the context of NMOR magnetometry, applied light needs to be tuned to a specific transition in magneto-optically active medium. In the case of alkali vapor, typically used in optical magnetometers, the light is tuned to the strongest D_1 or D_2 spectral lines (e.g., rubidium D_1—795 nm, rubidium D_2—780 nm, cesium D_1—894 nm, cesium D_2—852 nm, potassium—770 nm). This tuning needs to be performed with subpicometer precision. Moreover, due to the dependence of the NMOR signal on the wavelength, the wavelength needs to be stabilized over time with even better stability. This aim can be achieved with several techniques, e.g. absorption spectroscopy or magnetically induced dichroism or birefringence.

Another crucial characteristic required for the NMOR magnetometry of stronger fields is the modulation of light. With diode lasers, FM light can be generated by varying the laser current. This can be easily realized within a bandwidth of 0–1 MHz, which corresponds to the magnetic-field range spanning from ultra-weak to geophysical (or stronger) fields. The FM light may be also generated with external elements, e.g., electro-optical phase shifters. Application of AM light in NMOR

typically requires a use of external modulators.[7] Simplistic approach consists in mechanical chopping of the light beam. This approach, however, has serious drawbacks like: (1) narrow bandwidth of the light modulation and limited precision of frequency control, and (2) limited capabilities of the pulse shaping. Therefore, other approaches are used for AM modulation. One of them employs application of the acousto-optical modulators (AOMs). By varying the amplitude of radio-frequency signal driving the AOM, one may modulate the efficiency of the light diffraction. This enables modulation of light intensity in broad dynamic range and arbitrary shaping of light pulses. The drawback of the AOMs, however, is the power required for their operation (typically on the order of 10 W). To avoid this problem, waveguide-based modulators may be used. Such devices are based on a Mach-Zehnder interferometers with electro-optical modulators incorporated into interferometer arms. By changing the phase of interfering beams one can modulate the intensity of light. The advantages of such modulators are their flexibility in shaping of pulse characteristics and low power consumption. Additionally, the devices offer good integrability with other electronic components.

The last group of elements used for tailoring the light parameters in NMOR magnetometers are passive optical elements. In each system, such elements as mirrors, wave plates, polarizers, optical fibers are being used to direct light beam, control its polarization and intensity.

4.1.2 Field-Sensing Medium

In NMOR magnetometers, alkali-metal vapors are most commonly used as magneto-optically-active medium. Their main advantages are simple electronic structure, enabling manipulation of a single spin, excitability of spectral lines with available light sources (diode lasers), high vapor pressures at not-too-high temperatures. The vapors are contained in glass cells (typically made of Pyrex) of sizes ranging between 0.01 and 1000 cm^3 (with $\sim$1-cm^3 being a typical size of the vapor cell). The cells are often heated to several tens of Celsius, providing the vapor optical depth on the order of unity. The vapor heating, to enhance the NMOR-signal amplitude, is typically performed using electric heaters (typically doubly twisted wire producing very low magnetic field) or with hot water/air. To prolong the effective interaction time of light and atoms, the glass cell is filled with additional buffer gas, e.g., neon, xenon, or molecular nitrogen, or its walls are coated with special anti-relaxation layer (Sect. 3.1.1). The typical relaxation times in the vapor cells used in optical magnetometers are on the order of 10 ms.

[7]While, in general, intensity of light can be modulated by varying the diode-laser current, such modulation requires changing the current in a broad range. The current modulation would also introduce frequency modulation of light in a range strongly exceeding the width of optical transition light operates at. This disables the possibility of decoupling of one modulation type from the other but also complicates the stabilization of (mean) wavelength of light, introducing instabilities of the recorded NMOR signals.

4.1.3 Polarimeter

To measure the magnetic field, the polarization rotation needs to be precisely determined. In most NMOR magnetometers, the detection of light polarization is performed using a balanced polarimeter. The polarimeter consists of a crystal polarizer, e.g., Wollaston prism, and two photodiodes monitoring light intensities directed in respective channels of the polarizer. Orientation of the polarizer axis by 45° with respect to the incident light polarization and detection of the difference of two photocurrents of the photodiodes provide direct measure of polarization rotation

$$\begin{aligned} S \propto I_1 - I_2 &= I_0 \sin^2[45^\circ + \varphi(t)] - I_0 \sin^2[45^\circ - \varphi(t)] \\ &= I_0 \sin[2\varphi(t)] \approx 2I_0\varphi(t), \end{aligned} \tag{11}$$

where $I_{1,2}$ are the intensities of light directed in respective channels of the polarimeter and I_0 is the intensity of light illuminating the polarizer. Based on Eq. (11), one can conclude that higher probe-light intensity allows for larger NMOR signals. Moreover, as discussed in Sect. 3.1.1, higher probe intensity allows reduction of the shot-noise. It should be noted, however, that larger I_0 more significantly affects evolution of the medium (optical pumping with the probe), which results in deterioration of the polarization rotation $\varphi(t)$.

Alternatively to the polarimeter detection, the polarization rotation can be measured with a single polarizer, slightly tilted with respect to the axis of incoming polarimeter

$$S \propto I_1 = I_0 \sin^2[\varphi_0 + \varphi(t)], \tag{12}$$

where φ_0 is the small uncrossing angle relative to the initial light polarization before the atomic sample. Tilting of the polarizer allows one to differentiate between rotation in opposite direction.[8] While the second solution is easier to implement, the detected signal is, for small angle proportional to the uncrossing angle, constant component proportional to φ_0^2, but also linearly and quadratically proportional to the magneto-optical rotation $\varphi(t)$.

4.2 Electronics

To detect magnetic field, the photodiode signal needs to be processed. In NMOR magnetometers, this task can be realized in two ways: detection of the amplitude of

[8]If $\varphi_0 = 0$, than $S \propto I_1 = I_0 \sin^2 \varphi(t)$. Thus, the signals for rotations in opposite directions are indistinguishable and the modulation of light polarization at $2\omega_L$ observed in the high-field NMOR results in the signal modulation at $4\omega_L$.

NMOR signal demodulated at the first harmonic of the modulation frequency (passive mode) or by the measurement of the frequency of the detected signal (self-oscillating mode).

4.2.1 Amplitude and Phase Detection

In the passive mode (see discussion in Sect. 3.4), the photodiode signal is fed into a lock-in amplifier. The amplifier demodulates the signal at a specific (typically first) harmonic of the light modulation frequency ω_m. This allows one to determine the amplitude and phase of the signal and track its characteristics in resonance (e.g., $\omega_m = 2\omega_L$). The tracking is realized using a software algorithm, implemented on a computer controlling the reference generator, or by hardware, where adjustment of the modulation frequency is realized by, for example, phase-locked loop (PLL) and voltage controlled oscillator (VCO). In typical fields measurements, the lock-in integration time is larger than the transverse relaxation time T_2, which enables strong suppression of the noise and more precise determination of the resonance position.

4.2.2 Frequency Detection

Alternatively to the amplitude and phase detection in the passive mode, the time-dependent photodiode difference signal may be used to drive the light modulation in the self-oscillation mode. In this mode, the polarimeter output signal is first filtered, then phase shifted, and amplified. The processed signal is then feed into the modulation port of the light-source system. If the phase between the driving signal and the output signal is shifted by 90°, this solution allows for automatic tracking of all magnetic-field changes. In this mode, the magnitude of the magnetic field is determined by the detection of the frequency of the modulation signal.

5 High-Field NMOR Magnetometry

The experimental arrangement discussed in the previous section allows one to build a fully operational NMOR magnetometer. Depending on the parameters of the system, such as light intensity and wavelength, type and shape of modulation, magnetic-field inhomogeneity, etc., the system may offer different performance. Figure 10 shows an exemplary magnetic-field tracking signal obtained with NMOR magnetometer exploiting AM light and rubidium vapor as the field-sensing medium. The system was operated in the self-oscillation mode, where every several tens of seconds the magnetic field was changed significantly (~ 10 μT). As shown, after each step, the system instantly follows magnetic-field changes.

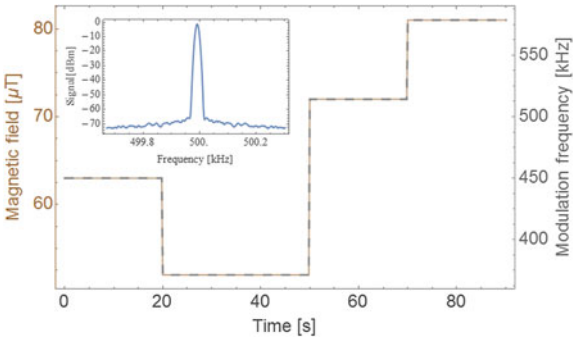

Fig. 10 Magnetic-field tracking signal. The *gray solid line* shows the detected modulation frequency of the self-oscillating system responding to the magnetic field (*dashed brown line*). Every time magnetic field was abruptly changed, the magnetometer momentarily adjusted its modulation frequency to the new resonance conditions. The *inset* shows the spectra of the signal recorded in the self-oscillating magnetometer for given conditions at magnetic field of 18.5 μT

The sensitivity of the measurement can be determined based on the SNR. Inset presents the square-root of the power spectral density of a magnetic field measured in semi-shielded magnetic-field environment (the end-caps at one side of the three-layer cylindrical mumetal magnetic shield were removed). At the spectrum, the strongest peak is observed at $\omega_m = 510$ kHz, which corresponds to the self-oscillating signal at a magnetic field of 18.5 μT ($\omega_L = 255$ kHz). From the Lorentz curve fitting to the peak and the noise floor observed in the spectrum (SNR $\approx$ 3500), we calculated the actual magnetometric sensitivity of the device $\sim$20 fT/Hz$^{1/2}$. This is roughly a factor of 10 larger than the corresponding fundamental sensitivity limit calculated based on Eq. (8). We attribute the deterioration of the sensitivity to a leakage of the uncontrollable magnetic field into the detection area, but also not-fully optimized conditions of the magnetometer operation.

A significant step in practical applications of NMOR magnetometer is its miniaturization. Figure 11 shows a picture of NMOR magnetometric head housing most of the optoelectronic component of the system. The head exists in two incarnations: (i) it is fully fiber coupled, i.e., light is remotely generated and

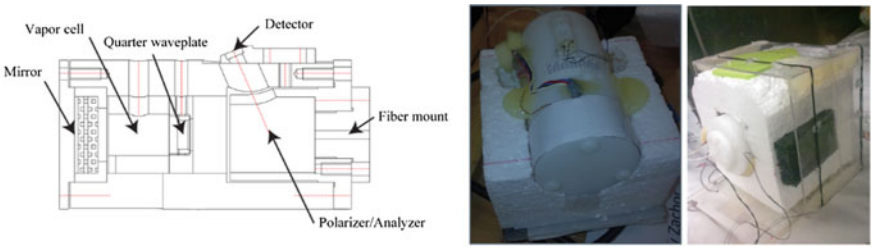

Fig. 11 A sensor head of a magnetometer exploiting AMOR

detected and it is delivered to and from the head through optical fibers and (ii) the diode laser and photodetectors are incorporated in the sensor head. While the first solution offers to remove all the metallic elements from the vicinity of the investigated magnetic-field source, the second is less demanding technical-wise (no need for coupling light into a single-mode polarization-maintaining fibers).

6 Conclusions and Outlook

Optical magnetometers have their roots in early discoveries in optics and magnetism. Progress in laser spectroscopy, optical pumping and understanding of quantum interference led to development of NMOR magnetometers as very useful and reliable instruments. The main advantages of the NMOR magnetometry which made this possible are: technical simplicity, high accuracy and wide dynamic range. The potential of these devices is exploited in ever-increasing area which spans from the basic science to many important practical applications.

References

1. M. Faraday, On the magnetization of light, and the illumination of magnetic lines of force. Philos. Trans. R. Soc. Lond. **1**, 104–123 (1846)
2. D. Macaluso, O. Corbino, Sopra una nuova azione che la luce subisce attraversando alcuni vapori metallici in un campo magnetico. Nuovo Cimento **8**, 257–258 (1898)
3. D. Macaluso, O.M. Corbino, L. Magri, Sulla relazione tra il fenomeno di Zeemann e la rotazione magnetica anomala del piano di polarizzazione della luce. Nuovo Cimento **9**, 384–389 (1899)
4. D. Budker, W. Gawlik, D.F. Kimball, S.M. Rochester, V.V. Yashchuk, A. Weis, Resonant nonlinear magneto-optical effects in atoms. Rev. Mod. Phys. **74**, 1153–1201 (2002)
5. E. Verdet, Recherches sur les proprietes optiques developpees dans les corps transparents par laction du magnetisme. Ann. Chim. Phys. **41**, 370–412 (1854)
6. L. Sun, S. Jiang, J.R. Marciante, Compact all-fiber optical Faraday components using 65-wt%-terbium-doped fiber with a record Verdet constant of-32 rad/(Tm). Opt. Express **18**, 12191–12196 (2010)
7. S. Li, P. Vachaspati, D. Sheng, N. Dural, M.V. Romalis, Optical rotation in excess of 100 rad generated by Rb vapor in a multipass cell. Phys. Rev. A **84**, 061403(R) (2011)
8. D. Sheng, S. Li, N. Dural, M.V. Romalis, Subfemtotesla scalar atomic magnetometry using multipass cells. Phys. Rev. Lett. **110**, 160802 (2013)
9. D. Jacob, M. Vallet, F. Bretenaker, A. Le Floch, R. Le Naour, Small Faraday rotation measurement with a Fabry-Perot cavity. Appl. Phys. Lett. **66**, 3546 (1995)
10. C. Cohen-Tannoudji, A. Kastler, Optical pumping, in *Progress in Optics*, vol V, ed. by E. Wolf, (Elsevier, North Holland, 1966), p. 1
11. G.W. Series, Optical pumping and related topics, in *Quantum Optics*, the 1969 Scottisch Universities Summer School, ed. by S.M. Kay, A. Maitland (Academic Press, London, 1970), p. 395
12. A. Corney, *Atomic and Laser Spectroscopy* (Oxford University Presss, Oxford, 1977)

13. W. Gawlik, J. Kowalski, R. Neumann, F. Träger, Observation of the electric hexadecapole moment of free Na atoms in a forward scattering experiement. Opt. Commun. **12**, 400 (1974)
14. W. Bennett, Hole burning effects in a He-Ne optical maser. Phys. Rev. **126**, 580 (1962)
15. W. Gawlik, S. Pustelny, Nonlinear Faraday effect and its applications, in *New Trends in Quantum Coherence*, ed. by R. Drampyan (Nova, New York, 2009), p. 47
16. D. Budker, D.F. Kimbal Rochester (eds.), *Optical Magnetometry* (Cambridge University Press, Cambridge, 2013)
17. D. Budker, V. Yashchuk, M. Zolotorev, Nonlinear Magneto-optic effects with ultranarrow widths. Phys. Rev. Lett. **81**, 5788 (1998)
18. W.E. Bell, A.L. Bloom, Optically driven spin precession. Phys. Rev. Lett. **6**, 280–281 (1961)
19. S. Pustelny, M. Koczwara, Ł. Cincio, W. Gawlik, Tailoring quantum superpositions with linearly polarized amplitude-modulated light. Phys. Rev. A **83**, 043832 (2011)
20. D. Budker, D.F. Kimball, S.M. Rochester, V.V. Yashchuk, Nonlinear magneto-optical rotation via alignment-to-orientation conversion. Phys. Rev. Lett. **85**, 2088 (2000)
21. D.F. Jackson Kimball, S. Pustelny, V.V. Yashchuk, D. Budker, Optical magnetometry with modulated light, in *Optical magnetometry*, ed. by D. Budker, F.D.J. Kimball (Cambridge University Press, Cambridge, 2013), pp. 104–124
22. Z.D. Grujić, A. Weis, Atomic magnetic resonance induced by amplitude-, frequency-, or polarization-modulated light. Phys. Rev. A **88**, 012508 (2013)
23. E. Breschi, Z.D. Gruijć, P. Knowles, A. Weis, Magneto-optical spectroscopy with polarization-modulated light. Phys. Rev. A **88**, 022506 (2013)
24. Y.P. Malakyan, S.M. Rochester, D. Budker, D.F. Kimball, V.V. Yashchuk, Nonlinear magneto-optical rotation of frequency-modulated light resonant with a low-*J* transition. Phys. Rev. A **69**, 013817 (2004)
25. W. Gawlik, L. Krzemień, S. Pustelny, D. Sangla, J. Zachorowski, M. Graf, A. Sushkov, D. Budker, Nonlinear magneto-optical rotation with amplitude-modulated light. Appl. Phys. Lett. **88**, 131108 (2006)
26. C.C. Gerry, P.L. Knight, *Introductory Quantum Optics* (Cambridge University Press, Cambridge, 2005)
27. M. Auzinsh, M. Auzinsh, D. Budker, D.F. Kimball, S.M. Rochester, J.E. Stalnaker, A.O. Sushkov, V.V. Yashchuk, Phys. Rev. Lett. **93**, 173002 (2004)
28. A.F. Molish, B.P. Oehry, *Radiation Trapping in Atomic Vapours* (Oxford University Press, Oxford, 1998)
29. J.P. Wittke, R.H. Dicke, Phys. Rev. **103**, 620 (1956)
30. W. Gawlik, Nonstationary effects in velocity-selective optical pumping. Phys. Rev. A **34**, 3760 (1986)
31. E. Pfleghaar, J. Wurster, S.I. Kanorsky, A. Weis, Time of flight effects in nonlinear magneto-optical spectroscopy. Opt. Commun. **99**, 303 (1993)
32. M. Erhard, H.-P. Helm, Buffer-gas effects on dark resonances: theory and experiment. Phys. Rev. A **63**, 043813 (2001)
33. M.V. Balabas, T. Karaulanov, M.P. Ledbetter, D. Budker, Polarized alkali-metal vapor with minute-long transverse spin-relaxation time. Phys. Rev. Lett. **105**, 070801 (2010)
34. V.G. Lucivero, P. Anielski, W. Gawlik, M.W. Mitchell, Shot-noise-limited magnetometer with sub-picotesla sensitivity at room temperature. Rev. Sci. Instr. **85**, 113108 (2014)
35. W. Wasilewski, K. Jensen, H. Krauter, J.J. Renema, M.V. Balabas, E.S. Polzik, Phys. Rev. Lett. **104**, 133601 (2010)
36. I. Novikova, A.B. Matsko, V.L. Velichansky, M.O. Scully, G.R. Welch, Phys. Rev. A **63**, 12 (2001)
37. G. Vasilakis, V. Shah, M.V. Romalis, Phys. Rev. Lett. **106**, 143601 (2011)
38. K. Jensen, V.M. Acosta, J.M. Higbie, M.P. Ledbetter, S.M. Rochester, D. Budker, Phys. Rev. A **79**, 023406 (2009)
39. D. Budker, D.F. Kimball, S.M. Rochester, V.V. Yashchuk, M. Zolotorev, Sensitive magnetometry based on nonlinear magneto-optical rotation. Phys. Rev. A **62**, 043403 (2000)

40. S. Pustelny, A. Wojciechowski, M. Gring, M. Kotyrba, J. Zachorowski, W. Gawlik, Magnetometry based on nonlinear magneto-optical rotation with amplitude modulated light. J. Appl. Phys. **103**, 063108 (2008)
41. W. Chalupczak, R.M. Godun, S. Pustelny, W. Gawlik, Room temperature femtotesla radio-frequency atomic magnetometer. Appl. Phys. Lett. **100**, 242401 (2012)
42. V.V. Yashchuk, S.-K. Lee, E. Paperno, Magnetic shielding, in *Optical Magnetometry*, ed. by D. Budker, D.F.J. Kimball (Cambridge University Press, Cambridge, 2013), pp. 104–124
43. S. Xu, S.M. Rochester, V.V. Yashchuk, M.H. Donaldson, D. Budker, Construction and applications of an atomic magnetic gradiometer based on nonlinear magneto-optical rotation. Rev. Sci. Instr. **77**, 083106 (2006)
44. S.J. Smullin, I.M. Savukov, G. Vasilakis, R.K. Ghosh, M.V. Romalis, Low-noise high-density alkali-metal scalar magnetometer. Phys. Rev. A **80**, 033420 (2009)
45. P. Wlodarczyk, S. Pustelny, J. Zachorowski, M. Lipinski, Modeling an optical magnetometer with electronic circuits-analysis and optimization. J. Instr. **7**, P07015 (2012)
46. S. Pustelny, W. Gawlik, S.M. Rochester, D.F. Jackson Kimball, V.V. Yashchuk, D. Budker, Nonlinear magneto-optical rotation with modulated light in tilted magnetic fields. Phys. Rev. A **74**, 063420 (2006)